Heat Transfer and Pressure Loss Characteristics of Very Compact Heat Sinks

by

Masahito Tasaka / Dr. Eng., Assistant Senior Research Engineer, Metal Working Process Research Dept., Corporate R & D Lab.
Chihiro Hayashi / Dr. Eng., Advisory Consultant, Head office
Toshio Aihara / Dr. Eng., Professor Emeritus, Institute of Fluid Science, Tohoku University

Synopsis

The present authors have developed high-performance and very compact heat sinks of both pin-fin and plate -fin types for air cooling manufactured using a patented wire-sawing machine, and experimentally studied their heat transfer and pressure loss characteristics. The present heat sinks with fin pitch of 0.4-2.1mm and thickness of 0.2-1.0mm have excellent cooling performance per unit heat sink volume of three to ten times as large as conventional heat sinks. The correlation of the Colburn j-factor/Fanning friction factor vs. the Reynolds number for the present heat sinks was found to have very similar tendencies to those of conventional large-size heat exchangers in spite of the heat sink's extreme compactness and leading edge effect.

1. Introduction

In LSI (largescale integrated circuit) packaging for microprocessors, heat-generation density has been increasing year by year[1]. Effective cooling of the LSI with high heat generation at a limited temperature difference between circuits and coolant is essential for maintaining reliability, long life, and controlling thermally induced stresses[2)~6)]. In order to keep the LSI junctions at a normal temperature, forced air cooling is generally used, and if the heat generation exceeds the ability of air-cooling, systems liquid cooling tends to be adopted[7),8)]. However, liquid cooling systems need complex pipelines with sealing/proof mechanisms and flow control systems; therefore maintenance of the system is not easy. Use of an air cooling system is desirable in next-generation LSI packaging. In general, air cooling is inferior to water cooling in terms of heat transfer performance.

Considering this problem, the present authors have developed high-performance and compact heat sinks for air cooling[9)~11)]. These highly compact heat sinks, having a fin pitch of 0.4-2.1mm and a fin thickness of 0.2-1.0mm, were manufactured by a newly developed wire-sawing machine[12),13)]. This patented machining method ensures mass production of extremely compact heat sinks with substantially lowar cost than photo-etching.

In this study, heat transfer and pressure loss characteristics of both pin fin and plate fin heat sinks were experimentally studied, and the measured values were compared with those of conventional commercial heat sinks having coarser fins. Along with these experimental results, an elementary design principle of a compact heat sink is also presented in the present report.

2. Experimental Apparatus and Procedure

In the present experiments, seven heat sinks were tested. Two of them were pin-fin typ heat sinks, and the others were of the plate-fin type. Outlines of these heat sinks are shown in **Fig. 1(a)** and **Fig. 1 (b)** with their geometries in **Fig. 2(a)** and **Fig. 2(b)**; their dimensions are listed in **Table 1**. All heat sinks were made of duralumin. Hereafter each heat sink is referred to as **P1**, **F1**, etc., as indicated in **Table 1**; **F0** corresponds to the commercial heat sink with the finest fins, and the other two heat sinks are called very compact heat sinks, which were made by the patented machining process.

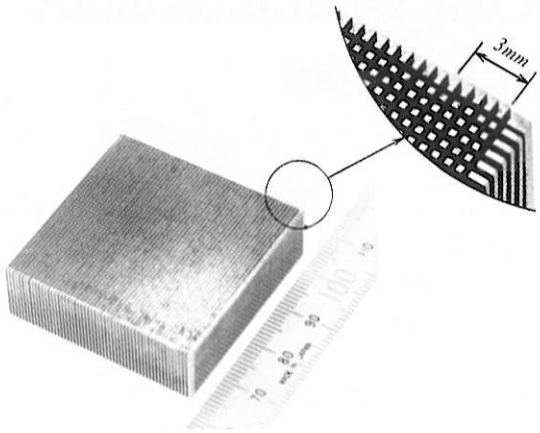

(a) Pin-fin type

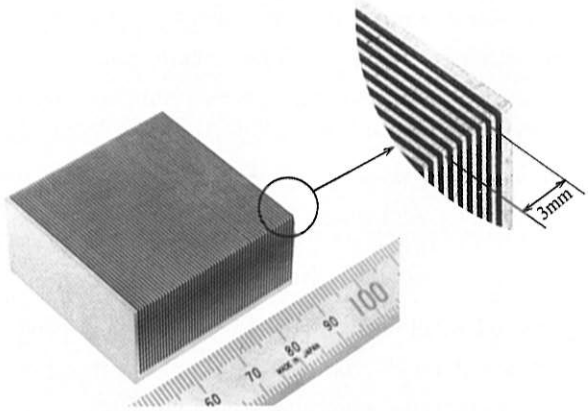

(b) Plate-fin type

Fig. 1 Outline of compact heat sinks

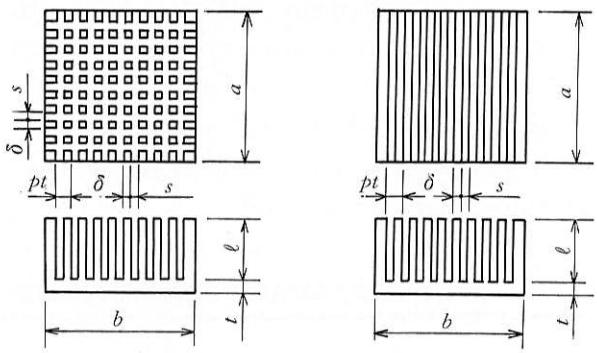

(a) Pin-fin type (b) Plate-fin type

Fig. 2 Geometry of heat sink

Figure 3 is an outline of the wind tunnel. First, room air was drawn into an inlet nozzle for measuring the volumetric air flow rate. The flow rate of a five-stage turbo blower was controlled by regulating its speed with an inverter. The test section was connected downstream of the blower, the vibration from which was cut off by flexible ducts.

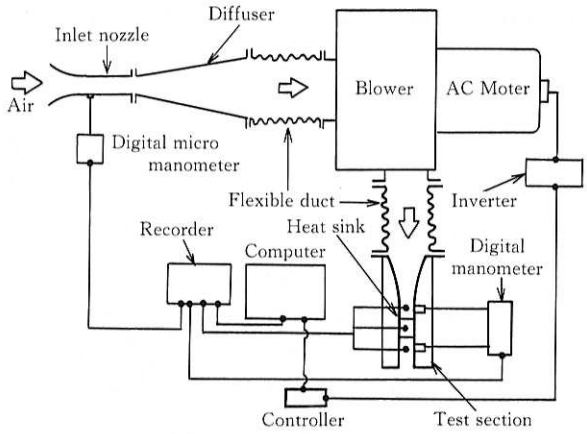

Fig. 3 Outline of wind tunnel
(Mark ● refers to a thermocouple.)

Figure 4 shows a schematic of the test section, in which two identical heat sinks were installed symmetrically. A sheet of nichrome heater was sandwiched between them. This construction was adopted in order to eliminate the heat leakage from the rear surface of the base plate, which was the main error source in the testing of heat sinks. The installed heat sinks have the same width and height as the test section duct, so as to prevent air leakage through the clearance between them. The temperatures of both base plates were measured with 76-μm-dia. copper-constantan thermocouples at six points, as shown in **Fig. 5**. The inlet and outlet air temperatures T_{a1} and T_{a2} were measured with 127-μm-dia. copper-constantan thermocouples. In particular, the outlet air temperature was measured

Table 1 Geometrical dimensions of test heat sinks

Symbol	Heat sink	pt	s	δ	a	b	ℓ	A	V_{fin}
●	P1	2.08	1.04	1.04	40	40	17.0	2.79	2.72
■	P2	0.70	0.34	0.36			16.5	8.02	2.64
○	F1	2.08	1.04	1.04			17.0	2.60	2.72
□	F2	0.70	0.34	0.36			16.5	7.43	2.64
△	F3		0.43	0.27	20		17.7	4.03	1.42
▽	F4						7.8	1.80	0.62
×	F0	4.30	3.00	1.30	40		18.0	1.37	2.88

(Unit : $\times 10^{-2}$m^2 for A, $\times 10^{-5}$m^3 for V_{fin} $\times 10^{-3}$m for others)

downstream of a mixer to obtain bulk value. The heat transfer rate per heat sink, $\dot{Q}$, was determined to be half of the electric power input to the sheet heater clamped by a pair of test heat sinks, from which the heat leakage through the thermal insulator was 1% or less of $\dot{Q}$. The average heat transfer coefficient h_{bs} is defined as

$$h_{bs}=\dot{Q}/(A_{bs}\cdot(\overline{T}_{bs}-\overline{T}_a)), \quad (1)$$

where $\overline{T}_{bs}$ is the average base plate temperature, determined as an arithmetic mean of the measured temperatures at the six points shown in **Fig. 5**. Pressure loss across the heat sink was measured at points 25mm upstream and 40mm downstream of the heat sinks.

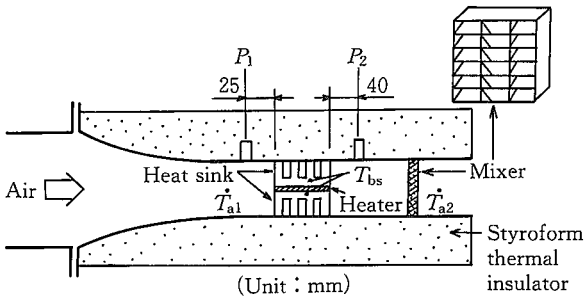

Fig. 4 Test section (Mark ● refers to a thermocouple.)

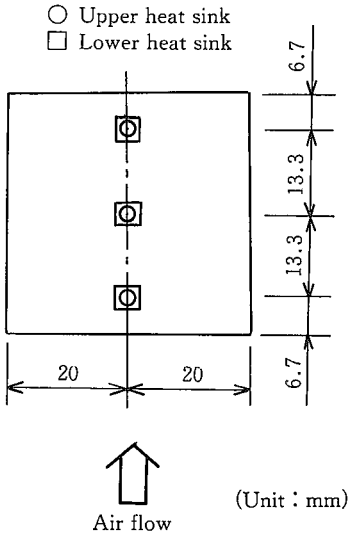

Fig. 5 Measuring points of base-plate temperature

3. Results and Discussion

3.1 Heat Transfer Coefficient

Figure 6 shows the effect of frontal air velocity u_{fr} on the heat transfer coefficient h_{bs}. The u_{fr} is defined as

$$u_{fr}=\dot{V}/(2b\cdot(\ell+t)). \quad (2)$$

As may be seen from the figure, the heat transfer coefficients for heat sinks **P1** and **F1** with 2.1mm fin pitch are three or four times as large as those for the commercial one, **F0**; the data on heat sinks **P2** and **F2** with 0.7mm fin pitch are six or seven times as large as those on **F0**. The improvement in heat transfer depends primarily on the increase of the heat transfer area. Comparison between the pin-fin type and plate-fin type shows that the heat transfer coefficient of **P1** becomes larger than that of **F1** with increasing air velocity $\mathbf{u}_{fr}$; however, there is little difference in the heat transfer coefficient between **P2** and **F2**, which have small fin pitch. The former tendency arises from the heat transfer augmentation by pin fins owing to the leading edge effect and the early transition to turbulent flow. The reasons for the latter tendency are that the heat sinks with fine pin pitch lose such merits in exchange for the largely extended surface area, and that the fin efficiency of pin fins is lower than that of a plate fin.

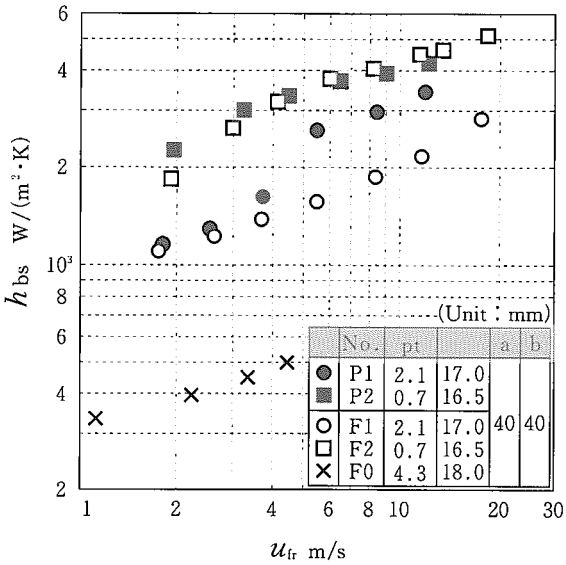

Fig. 6 Effect of frontal air velocity on heat transfer coefficient

Figure 7 shows the effect of the streamwise length a and height of plate fin on the average heat transfer coefficient h_{bs}. Comparison between the **F2** and **F3**, having the same fin height but different streamwise length, shows that although the heat transfer coefficient of **F2** is smaller than that of **F3** at a low air velocity, that for **F2** becomes larger than that for **F3** as the air velocity is increased. The

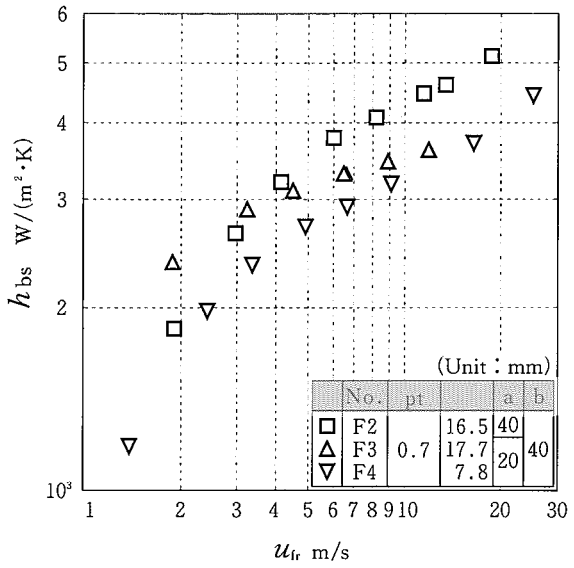

Fig. 7 Effect of fin length and fin height on heat transfer coefficient

reason for this is as follows: In the low-velocity range, the temperature efficiency is nearly unity; consequently the downstream part of the **F2** fins does not act effectively as an extended heat transfer surface. However, with an increase in the air velocity, the temperature efficiency is reduced, and then the downstream part of the fin also becomes efficient. On the other hand, in comparison of **F3** with **F4**, both of them having the same streamwise length but different fin height, the heat transfer coefficient of **F3** is greater than that of **F4** in a low-velocity range, while they are almost identical in a high-velocity range. This tendency seems to be caused by a decrease in fin efficiency with increasing air velocity.

3.2 Compactness Factor

Recently the size of LSI modules has become extremely small and the heat generation density in the modules is very high. Therefore it is of practical importance to dissipate such a large amount of heat in a limited space. Thus, the compactness factor is newly introduced here in order to evaluate the heat dissipating performance per unit heat-sink volume. The compactness factor ϕ_c is defined as

$$\phi_c = \dot{Q}/(V_{fin} \cdot (\overline{T}_{bs} - T_{a1})), \quad (3)$$

where T_{a1} is the measured inlet air temperature, and V_{fin} is the volume occupied by the finned part (not including the base plate) of a heat sink, which is calculated as $a \cdot b \cdot \ell$.

The compactness factors evaluated for the five plate-fin-type heat sinks tested are plotted in **Fig. 8**. All the compact heat sinks, **F1**, **F2**, **F3**, and **F4**, have values about three to nine times as large as the commercial type **F0**. It may be concluded from the result that minimizing the fin pitch is very effective in improving the heat-sink compactness. As for the compactness factor of **F2** and **F3**, a similar tendency to that shown in **Fig. 7** is also observed. The compactness factor for heat sink **F4** with half the streamwise length and half the fin height of **F2** is twice as large as that for heat sink **F2**.

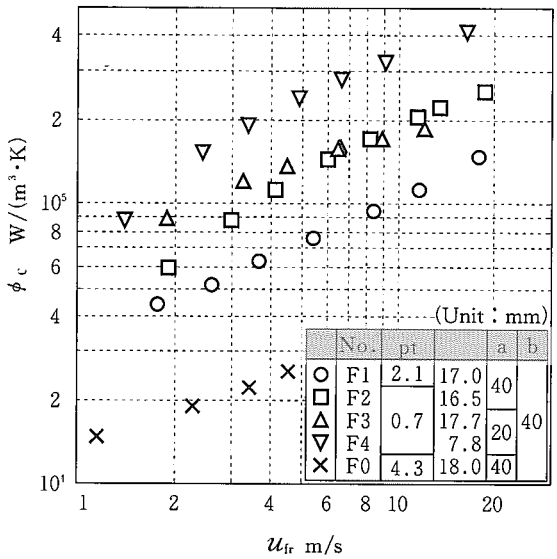

Fig. 8 Effect of air velocity and fin size on compactness factor

3.3 Pressure Loss

Figure 9 is a plot of the pressure loss. Δp vs. frontal air velocity for the seven heat sinks tested. It is natural, considering the difference in the fin pitch pt and streamwise length, that the present compact heat sinks should produce a larger pressure loss than the **F0** type and that short heat sinks **F3** and **F4** show a much smaller pressure loss than the other heat sinks. However, it should be noted that the plate-fin type produces a lesser pressure loss than the pin-fin type at a higher velocity range, because there is no separation in the channels.

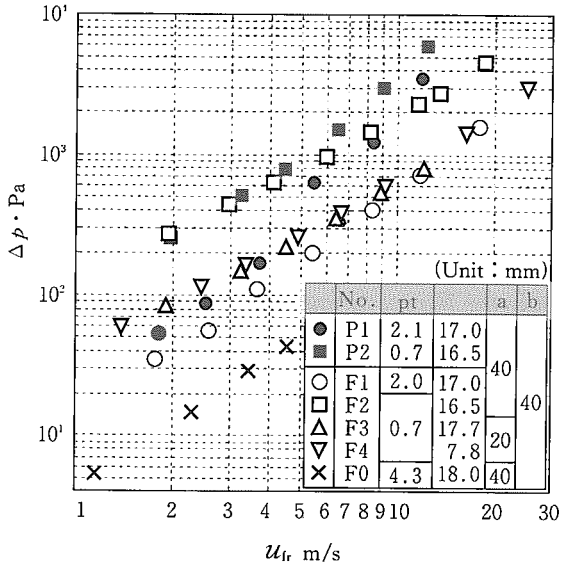

Fig. 9 Effect of air velocity on pressure drop

3.4 Overall Evaluation of Heat Sink

In forced air cooling of a LSI module, the power consumption and noise of a fan/blower cannot be ignored. Therefore, it is very important in practical use to take into account the relation between the cooling performance and the blower power consumption[9),10),14),15),16)]. **Figure 10** is a plot of the compactness factor ϕc against the air blowing power $\Delta p \cdot \dot{V}$. As can be seen from the figure, the compact heat sinks have two to ten times as great compactness as the commercial-type **F0**. These results show that heat sinks with a fine fin pitch are still more advantageous in terms of cooling performance than those with a coarse fin pitch, in spite of the large pressure loss due to narrow fin spacing. Among the six compact heat sinks tested, type **F4** has a compactness factor three or four times as large as the other types, **P1**, **P2**, **F1**, and **F2**; on the other hand, the compactness factor for type **F3** is almost twice those for the other four types in a small power consumption range. This suggests that the compactness factor per blower-power consumption can be improved by making the heat-sink volume small and the fin and its pitch fine.

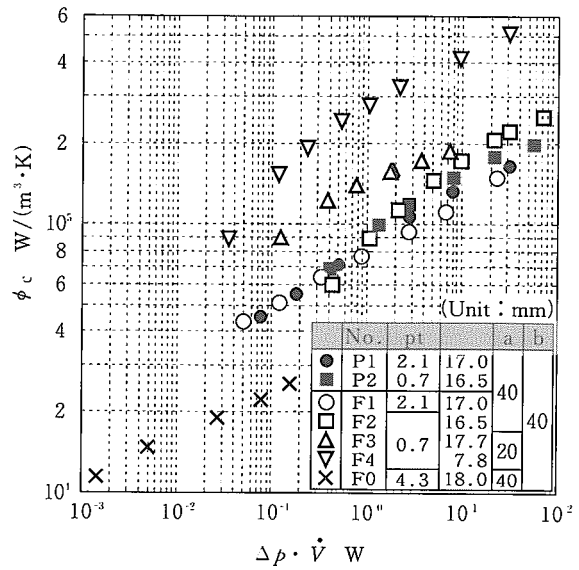

Fig. 10 Effect of blower power consumption on compactness factor

The Colburn j-factor and Fanning friction factor f, defined by equations (4) and (5), have generally been used in the evaluation of the heat exchanger performance. Both of them are plotted in **Fig. 11** and **Fig. 12** versus the Reynolds number Re along with the data on compact heat exchangers from the book by Kays and London[17)].

$$j = Nu/(Re \cdot Pr^{1/3}), \quad (4)$$

$$f = 2 \cdot r_h \cdot \Delta p/(\rho \cdot u_c^2 \cdot a), \quad (5)$$

where

$$Re = 4 \cdot r_h \cdot u_c/\nu,\ Nu = 4 \cdot r_h \cdot h/\lambda,\ r_h = A_c \cdot a/A,$$

$$u_c = \dot{V}/A_c, \quad (6)$$

$$h = \dot{Q}/(A \cdot \eta \cdot (\overline{T}_{bs} - \overline{T}_a)). \quad (7)$$

The average air temperature $\overline{T}_a$ is the arithmetic mean of the inlet and outlet air temperatures. The fin efficiency η is calculated by equation (8) on the assumption of one-dimensional heat conduction in a fin, and constant heat-transfer coefficient as,

$$\eta = \tanh(m \cdot \ell)/(m \cdot \ell), \quad (8)$$

$m = \sqrt{4 \cdot h/(\delta \cdot \lambda)}$ for pin-fin type,

$m = \sqrt{2 \cdot (\delta + a) \cdot h/(\delta \cdot a \cdot \lambda)}$ for plate-fin type.

The j and f factors are plotted for the pin-fin heat sinks in **Fig. 11**, where the data on a compact heat exchanger surface are also replotted from Table 10 -7 of Kays and London[17)]. Hereafter, their data on pin-fin and plate-fin surfaces are referred to as K-L. **Figure 12** is a plot of the j and f factors for the plate-fin heat sinks and the plain plate-fin surface. The latter data, K-L, are replotted from Table 10-3 of Kays and London[17)]. Although the present heat sinks have a much smaller fin pitch, and the pin-fin type especially has a considerable leading-edge effect compared with the K-L heat exchanger, the relations of j and f vs. the Re for the compact heat sinks are virtually identical to those of the K-L data. Furthermore, a good analogy between the j and f factors is also recognized for the compact

heat sinks. This is a very useful finding for optimum heat-sink design. The variational tendency of the friction factor of type **P1** suggests that the transition of flow from laminar to turbulent occurs nearly at Re=1 000. This transition Reynolds number is almost half of the normal value. This can be attributed to free-stream turbulence upstream of the heat sinks; the measured turbulence intensity of the main stream was six or ten percent over the experimental range of u_{fr}=1-30 m/s. Since the fin efficiency of types **P2**,**F2** and **F3** is very small, their Colburn j-factor is lower than those of other compact heat sinks.

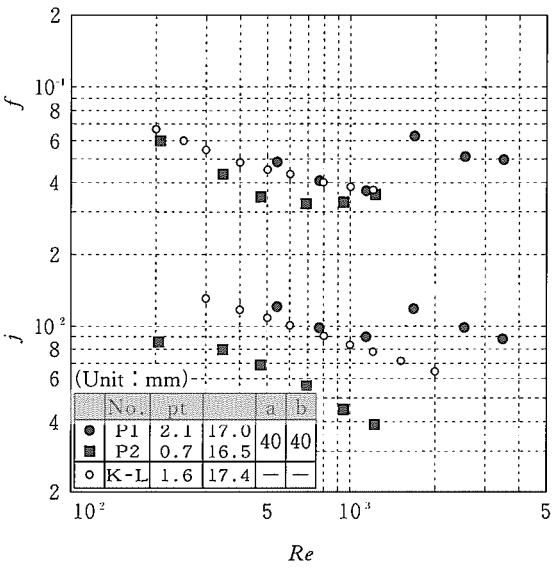

Fig. 11 Colburn j-factor and Fanndng friction factor f vs. Reynolds number (pin-fin type)

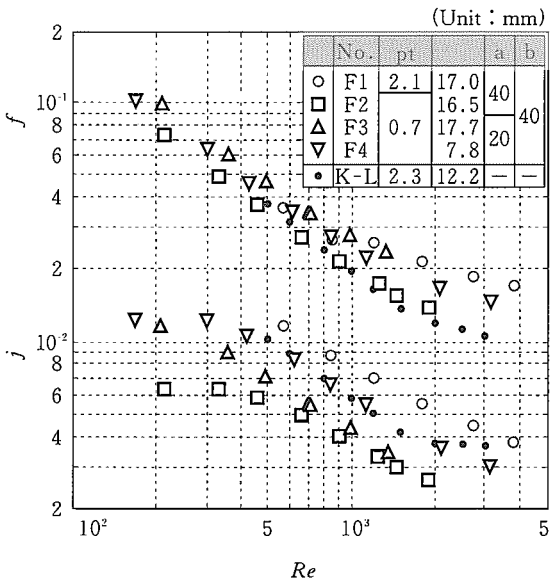

Fig. 12 Colburn j-factor and Fanning friction factor f vs. Reynolds number (plate-fin type)

3.5 Optimum Design Principle

Generally, a fan/blower has a peculiar relationship between the volumetric flow rate and delivery static pressure. Therefore, the operating point $\dot{V}$ of a cooling system is determined by a balance between the static pressure rise p_s and the pressure loss Δp across the heat sinks, as shown in **Fig. 13 (a)**. In the figure, the measured pressure-loss curves for the plate-fin heat sinks of three types and the assumed performance curves for two types of blower are given; all combinations of the p_s-curves and Δp-curves give six operating points A, B, C, G, H and I as their respective points of intersection. If the fin pitch is decreased to obtain a larger heat-transfer area, then the operating point shifts towards the range of less air-flow rate, owing to a rise of pressure loss.

In **Fig. 13(b)**, the compactness factor ϕ_c corresponding to each operating point A, B, C, G, H and I is indicated as points D, E, F, J, K and L. It can be seen from inspection of the figure that the heat sink **F4** shows the highest compactness among all the combinations, and **F1** shows approximately three times higher compactness than the commercial type **F0**, in spite of the reduction in air flow rate due to the increased pressure loss.

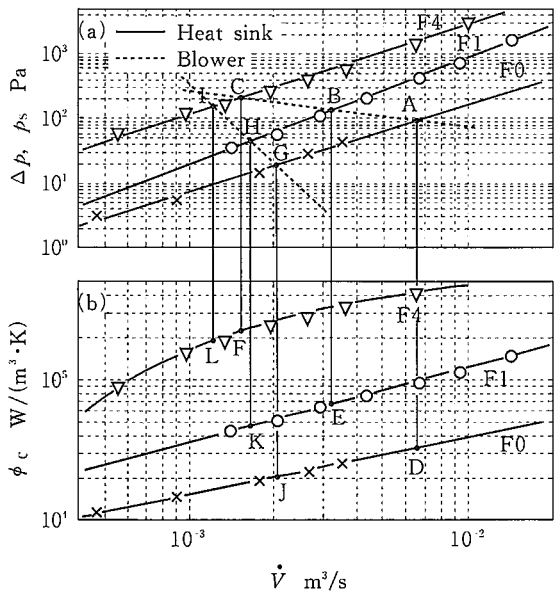

Fig. 13 Optimum design of heat-sink cooling system (a)Heat-sink pressure drop Δp and blower delivery pressure p_s, (b)Compactness factor ϕ_c

4. Concluding Remarks

Air-cooled, very compact heat sinks of both pin-fin and plate-fin types were developed for electronic packaging/LSI with high heat generation density, and their heat transfer and pressure loss characteristics were studied experimentally.

The present compact heat sinks with extremely fine fins have excellent characteristics in terms of compactness factor, defined as heat dissipating performance per unit heat-sink volume. The heat sink with the most outstanding performance among those tested showed a compactness factor seven to ten times as large as that of the commercial heat sink with the highest performance in current use; even the low-performance heat sink still has a compactness factor three times larger than the commercial one.

The present experiment further clarified the following. The correlation of the Colburn j-factor/Fanning friction factor f vs. the Reynolds number for the present heat sinks were found to be very similar to those of conventional large-size heat exchangers, in spite of the extreme compactness and leading edge effect. This finding gives us useful information for optimum design of high-performance heat sinks. Finally, basic design principles for a heat sink cooling system are proposed, taking into consideration the pressure loss characteristics of a heat sink and the delivery pressure and discharge rate performance of a fan/blower.

Nomenclature

A_{bs} : base-plate area of heat sink, m^2
a : streamwise length of heat sink, m
b : width of heat sink, m
C : thermal conductance, W/K
h_{bs} : average heat transfer coefficient, based on the base-plate area, $W/(m^2 \cdot K)$
ℓ : fin height, m
Δp : pressure loss across a heat sink, Pa
pt : fin pitch, m
$\dot{Q}$: rate of heat transfer, W
s : fin spacing, m
$\overline{T}_a$: arithmetic mean of inlet/outlet air temperatures, K
T_{a1} : inlet air temperature to heat sink, K
T_{a2} : outlet air temperature from heat sink, K
T_{bs} : mean base-plate temperature, K
u_{fr} : frontal air velocity, m/s
$\dot{V}$: volumetric air flow rate, m^3/s
V_{fin} : volume occupied by finned part of a heat sink, m^3
δ : fin thickness, m
ϕ_c : compactness factor, $W/(m^3 \cdot K)$

Masahito Tasaka

Dr. Eng., Assistant Senior Research Engineer, Metal Working Process Research Dept., Corporate R & D Lab.

Phone: 06(489)5717

References

1) Chu, R. C. et al., Advances Cooling Techniques for Computers, (1991), p.365, Win Aung ed., Hemisphere Pub.
2) Hannemann, R. et al., Advances Cooling Techniques for Computers, (1991), p.245, Win Aung ed., Hemisphere Pub.
3) Mahalingham, M. and Andrews, J., Cooling Technology for Electronic Equipment, (1988), p.139, Win Aung ed., Hemisphere Pub.
4) Knickerbocker, J. U. et al., IBM J. Res. and Dev., 35 (1991), p.330
5) Gani, V. L. et al., IBM J. Res. and Dev., 35 (1991), p.342
6) Oktay, S. et al., Proc. of IEEE Int. Conf. on Computer Design, (1983),
7) Hwang, U. P. et al., Proc. of the joint ASME/JSME advanced in Electronic Packaging, 1 (1992), p.75
8) Okano, M. et al., NEC Technical Report, 40 (1987), p.40, (in Japanese)
9) Ohara, T. et al., Proc. of the joint ASME/JSME advanced in Electronic Packaging, 1 (1992), p.249
10) Tasaka, M. et al., Proc. of 4th ASME/JSME Thermal Eng. Joint Conf., 4 (1995). p.223
11) Tasaka, M. et al., Proc. of 3rd KSME/JSME Thermal Eng. Conf., 1 (1996). p.553
12) Japan Patent Number Toku-kou-hei 04-29512
13) Japan Patent Number Toku-kou-hei 05-20227
14) Aihara, T. et al., Trans. JSME, Ser. B, 61 (1995), p.312, (in Japanese)
15) Bejan, A., ASME J. Heat Transfer, 99 (1977), p.374
16) Soland, J. et al., ASME J. Heat Transfer, 100 (1978), p.514
17) Kays, W. M. and London, A. L., Compact Heat Exchangers, 2nd Edition, (1964) , p.167, 176, 196, 217, McGraw Hill